

## Optical Microphone as Laser-Ultrasound Detector

Wolfgang Rohringer<sup>1</sup>, Thomas Heine<sup>1</sup>, Ryan Sommerhuber<sup>1</sup>, Nico Lehmann<sup>2</sup>, Balthasar Fischer<sup>1</sup>

<sup>1</sup> XARION Laser Acoustics GmbH, 1030 Wien, Austria, Email: w.rohringer@xarion.com

<sup>2</sup> Porsche Leipzig GmbH, 04158 Leipzig, Austria

The steadily increasing use of complex composite parts for production, such as fiber-reinforced composite components, and the demand for fully automatized quality control in automotive and aerospace industry promote a need for non-contact non-destructive testing (NDT) techniques [1, 2]. Due to its flexibility and the ability to reveal internal defects such as delaminations or cracks, ultrasound is one of the most widely used testing techniques [3]. Here, we present a novel non-contact non-destructive testing setup based on laser excitation of ultrasound and detection with a broadband, air-coupled optical microphone [4], allowing the cost-effective implementation of compact, fiber-coupled NDT probes for single-sided testing.

### Non-contact ultrasound testing using lasers

So far, most efforts towards non-contact ultrasound testing employ either on air-coupled ultrasound using piezoelectric transducers arranged in through-transmission mode, or optical excitation and detection of ultrasound with suitable lasers (Laser Ultrasonics, LUS) [5]. The absorption of nanosecond-timescale laser pulses generates extremely short ultrasound transients, either via ablation or thermoelastic expansion and subsequent relaxation [6]. These transients cause well-defined echoes, which can be separated with high temporal resolution, allowing for single-sided testing with a sufficiently broadband detection method. Today, this is usually realized by relying on the measurement of surface vibrations with suitable optical interferometers, offering detection bandwidths in excess of 100 MHz [7].

A disadvantage of this Laser Ultrasonics implementation is that its performance strongly depends on the optical properties as well as on the surface characteristics of the sample under test, both for excitation and for detection. Strongly scattering surfaces, for instance, require high-powered detection lasers and complex interferometer setups, which may be costly and difficult to miniaturize [8].

In this work, we present an alternative method based on air-coupled detection of laser-generated ultrasound with a broadband optical microphone. While the detection bandwidth in this setup is limited by ultrasound attenuation in air [9] to a range of 10 Hz up to 1 MHz, it is still a factor 10 larger than what state-of-the-art air-coupled piezo transducers can offer. Consequently, ultrasound transients with single-microsecond durations can be reliably detected, temporally separated and spectrally analyzed.

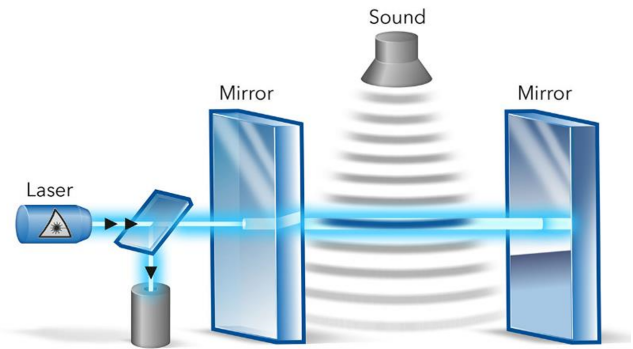


**Figure 1:** Optical microphone: detection principle. The wavelength of light in a medium depends on its refractive index, which is a function of the local density. Since sound modulates the density, it also modulates the optical wavelength, which can be detected with a rigid Fabry-Pérot etalon. The intensity reflected by the etalon depends on the wavelength of the laser in the medium between the mirrors, which is measured with a photodiode.

The air-coupled detection mechanism functions regardless of surface characteristics and optical properties of the sample. While it is especially well-matched to fiber-reinforced composite materials, and especially sandwich structures, where ultrasound propagation at frequencies higher than 1 MHz is typically strongly attenuated, the measurements presented in the following demonstrate its usefulness for non-destructive testing of steel parts.

### Optical microphone for air-coupled ultrasound detection

The detection principle of the optical microphone [10] is illustrated in Figure 1. Soundwaves modulate the density ( $\rho$ ) of a medium, and therefore also its optical refractive index ( $n$ ). In a medium, the wavelength of light ( $\lambda$ ) depends on the refractive index as

$$\lambda(n) = \frac{c}{n(\rho)f} = \frac{\lambda_0}{n(\rho)}, \quad (1)$$

where  $f$  denotes the frequency,  $c$  the speed of light and  $\lambda_0$  the vacuum wavelength. This means that a monochromatic laser beam propagating through the medium in the presence of a sound field undergoes a small modulation of its optical wavelength, proportional to the local density, and therefore, sound pressure. The core element of the optical microphone used to detect this wavelength modulation is a miniaturized, rigid Fabry-Pérot cavity consisting of two semireflective mirrors. The intensity of laser light reflected from such a cavity is given by the

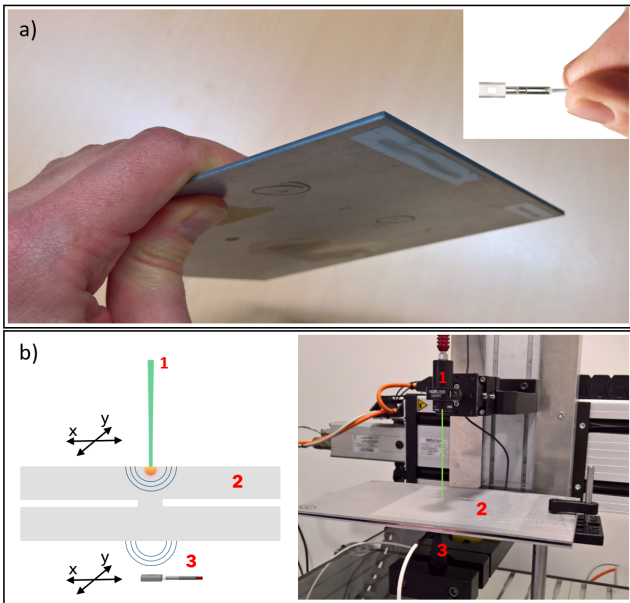


**Figure 2:** Sample used for measurements and detection setup. (a) All measurements have been performed on a spot welding sample consisting of two welded steel plates with dimensions of 20 cm by 20 cm and 1 mm thickness. Inset: optical microphone. (b) Through-transmission detection setup. Left panel: schematics; right panel: actual detection setup. 1: fiber-coupled excitation laser head, 2: sample, 3: optical microphone. Both the laser head and the sample were scanned to generate C-scans.

product of the input intensity  $I_0$  and a transfer function  $T_R(q)$ , which is given by the Airy function (see for instance [11])

$$T_R(q) = 1 - \frac{1}{1 + F \cdot \sin\left(\frac{q}{2}\right)^2}, \quad (2)$$

with the finesse coefficient  $F = 4R/(1 - R)^2$  and mirror reflectivity  $R$ . The round trip phase shift  $q$  depends on the laser wavelength  $\lambda(n)$  and the mirror distance  $d$  as

$$q(n) = \frac{4\pi d}{\lambda(n)} = \frac{4\pi n d}{\lambda_0}. \quad (3)$$

Therefore, any change in the laser wavelength induced by the sound field causes a change of the light intensity reflected by the cavity according to equation 2, which can be detected by a photodiode.

It is important to note that the mirror distance  $d$  is completely fixed; no mechanical movement or deformation takes part in the detection process that would limit the detection bandwidth, and no inert mass limits the impulse response or causes ringing. Light is coupled to the sensor via a fiber-optical cable connected to a remote unit containing the laser, control and detection electronics. Hence, the sensor head is a passive optical element, immune against electromagnetic interference on both sensor head or cable.

As shown in figure 2, the optical microphone has small dimensions (5 mm diameter), allowing integration into NDT probes with small footprints.

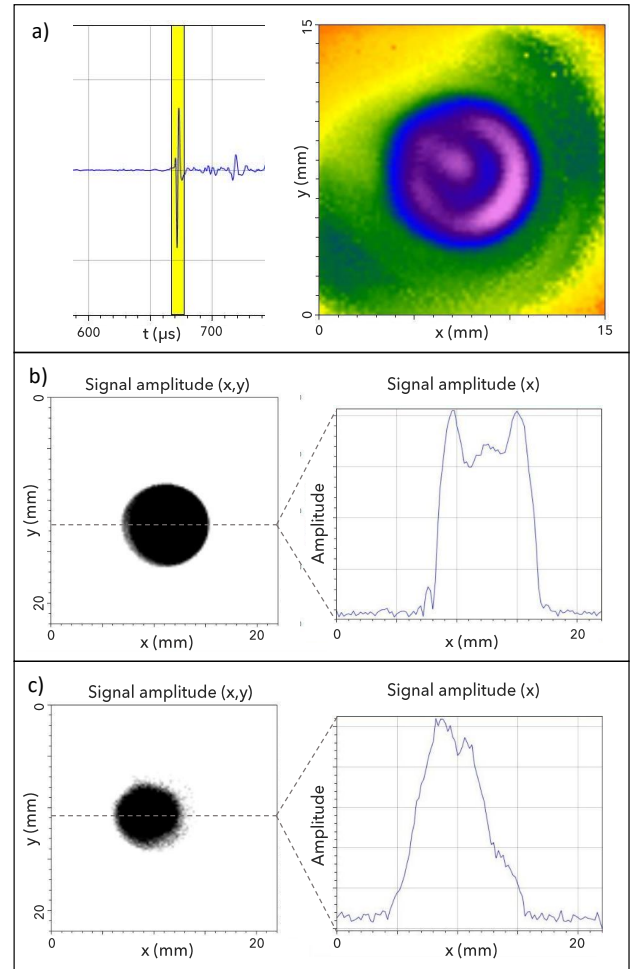


**Figure 3:** Results of the through-transmission measurements. (a) Typical time signal and C-scan of the spot weld. (b) Thresholded C-scan and line scan along x-axis of a good weld. The dashed line indicates the line scan position. (c) Thresholded C-scan and line scan along x-axis of a bad weld with too small diameter.

The optical microphone has been successfully deployed previously for various process control and non-destructive testing applications [12], as well as for photoacoustic microscopy in biomedical imaging [13]. In the following, the combination with laser excitation for non-destructive testing is demonstrated both for through-transmission as well as single-sided measurements.

### Through-transmission testing of spot welds

Figure 3(b) shows such a C-scan image of a spot weld. The connection formed by the weld guarantees good ultrasound transmission, while the surrounding gap strongly attenuates ultrasound propagation. The small detection area ( $0.3 \text{ mm} \cdot 2 \text{ mm}$ ) of the optical microphone results in a high lateral resolution. Figure 3(a) depicts a typical time signal from the dataset. It is characterized by a primary pulse of  $< 2 \mu\text{s}$  duration and demonstrates the bandwidth and time resolution which can be achieved in this setup.

All measurements presented here were performed on the

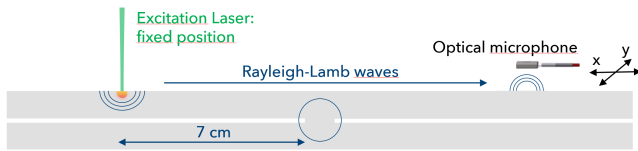


**Figure 4:** Schematics of the single-sided measurement setup. The excitation laser was delivered to a fixed point on the sample at a 7 cm distance to the spot weld. The optical microphone was positioned on the same side of the sample and scanned across a 5 cm by 5.5 cm imaging region containing the spot weld to detect guided waves propagating along the plate.

sample depicted in figure 2(a). It consists of two steel sheets with dimensions of 20 cm by 20 cm and 1 mm thickness, connected via a number of spot welds of varying quality and surface finish. The first set of measurements were performed in a through-transmission setup as outlined in figure 2(b) and shown in figure 2(c). The excitation laser was delivered by a compact fiber-coupled head that was mounted above the sample, while the optical microphone was placed at an approximately 1 cm distance below the sample. Both the excitation laser head and the microphone were scanned across the imaged area by a 2d scanning robot, and the locally detected ultrasound amplitudes were recorded to form a C-scan image in maximum amplitude projection.

For inline NDT, realistic testing times are usually limited to a few seconds. Therefore, it is useful to consider line scans through the spot welds. As an example, figure 3 shows a comparison between line scans through a good (b) and insufficient (c) weld that were recorded within a few seconds. The smaller extension of the bad spot weld (as quantified by the full width at half maximum (FWHM) of the line scan, for instance) is readily detectable.

### Single-sided testing of spot welds using Lamb waves

Sufficient bandwidth for temporal resolution of short ultrasound transients such as shown in figure 3(a) opens up the capability of non-contact single-sided testing. In this context, the use of Lamb waves for defect characterization, but also sample parameter estimation, is an active area of both scientific and industrial interest [14]. In the following, we present first measurements of the propagation of Lamb waves, generated by laser excitation in the vicinity of the spot weld, recorded with the optical microphone. For these measurements, the optical microphone and the excitation laser head were placed at the same side of the sample, as outlined in figure 4. The excitation laser was delivered to the plate at a fixed position, at a 7 cm distance to the point weld. The optical microphone was scanned over a 5 cm by 5.5 cm sized area containing the spot weld. A typical time signal is shown in figure 5(a). After a short time-delay, a signal associated with a guided wave is detected. At later times, this signal is superimposed with a high-amplitude signature

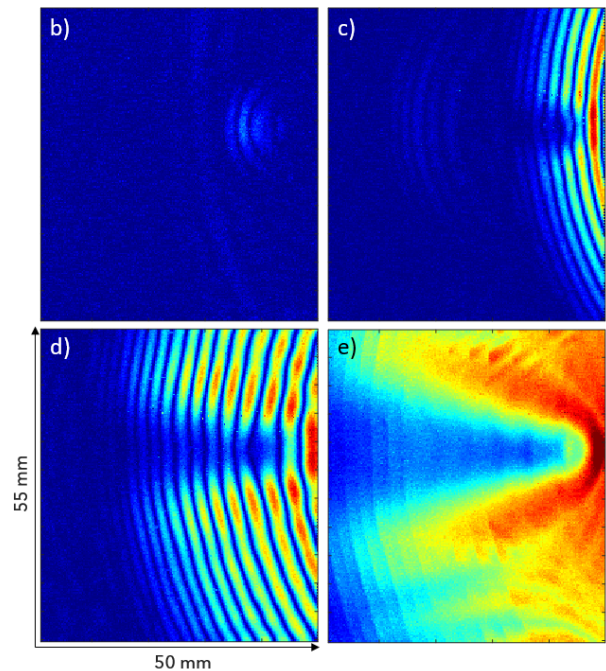
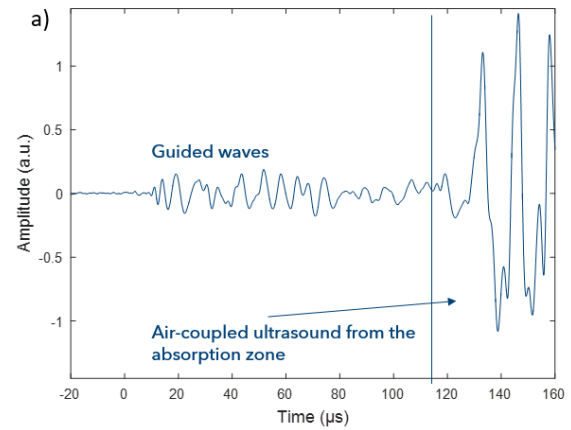


**Figure 5:** Results of the single-sided measurements. (a) Typical time trace showing a guided wave within the first 110  $\mu\text{s}$  and later arrival of an air-coupled signal from the excitation spot. (b)-(d) Time evolution of the guided wave. (b)  $S_0$  wave and  $A_0$  component from the spot weld. (c), (d) diffraction of an  $A_0$  mode around the spot weld. (e) Maximum amplitude projection over 20  $\mu\text{s}$  span showing the amplitude distribution around the weld.

associated with airborne ultrasound from the interaction point between the excitation laser and the plate.

The time evolution of the guided wave can be visualized in terms of C-scans of the signal amplitude at different points in time. Figure 5(b)-(d) shows such an image sequence, with 8  $\mu\text{s}$  time delay between each of the images. They show a primary  $S_0$  mode and an  $A_0$  component either accelerated by or generated at the spot weld due to mode conversion (b), and subsequent formation of a diffraction pattern around the point weld for a high-amplitude primary  $A_0$  mode generated by the laser absorption (c,d). The last panel (e) contains the maximum amplitude projection within a 20  $\mu\text{s}$  time window, showing the 'shadow' cast by the point weld, i.e. significantly reduced amplitude of the  $A_0$  mode behind the weld. Fu-



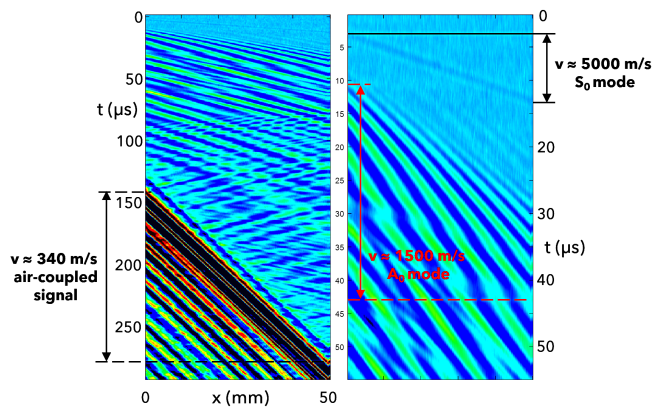


**Figure 6:** B-scan to identify observed modes based on their propagation velocity. The sensor was scanned over a 50 mm distance aligned with the excitation spot. Left panel: 290  $\mu\text{s}$  time segment containing the guided wave as well as the air-coupled signal at late times. Right panel: Zoom to the first 55  $\mu\text{s}$ , allowing the phase velocity estimation for two Lamb modes identified as  $A_0$  and  $S_0$  mode.

ture work will focus on utilizing the observed features for defect detection and characterization.

Finally, figure 6 shows a B-scan generated from time signals out of a line-scan along the x-axis, where the optical microphone was moved away from the source. From this B-scan, the propagation velocity of different observed modes can be estimated. Besides the air-coupled signal at later times, we identify a pronounced mode with a propagation velocity of  $v_{A_0} \approx 1500$  m/s as well as a low-amplitude mode ( $v_{S_0} \approx 5100$  m/s). By comparison with phase velocity values from published dispersion relations for thin steel plates [15], these modes can be identified as the lowest-order antisymmetric and symmetric  $A_0$  and  $S_0$  - modes, respectively, since higher-order modes with similar sound velocities only arise at frequencies beyond our measurement range. Future work will include the recovery of dispersion relations from B-scans via 2d FFT or wavelet analysis for parameter estimation, or to identify mode-conversion effects indicating the presence of defects.

## Summary and outlook

A novel non-contact non-destructive testing setup based on the combination of laser excitation with an air-coupled optical microphone has been presented. This combination allows for the implementation of compact, fiber-coupled NDT probes suited for the detection and generation of  $\mu\text{s}$ -timescale ultrasound transients. It has been demonstrated for both through-transmission as well as single-sided characterization of spot welds in steel. Both setups allow high-resolution imaging of defects. In the context of single-sided measurements, the propagation of Lamb-waves in the vicinity of the spot weld has been investigated. Future work will encompass measurements on different kind of sample materials and geometries, as well as the application-specific development of fast inline NDT setups.

## References

- [1] Gardner, W.E: Improving the effectiveness and reliability of non-destructive testing. International series on materials evaluation and non-destructive testing. Pergamon Press, Oxford, 1992
- [2] Heida, J.H., Platenkamp, D.J.: Evaluation of Non-Destructive Inspection Methods for Composite Aerospace Structures. 6th NDT in Progress, International Workshop of NDT Experts (2011)
- [3] Krautkrämer, J., Krautkrämer, H.: Ultrasonic testing of materials. Springer, Berlin Heidelberg, 1983
- [4] Fischer, B.: Optical microphone hears ultrasound. Nature Photonics 10 (2016), 356-358
- [5] Green, R.E.Jr.: Non-contact ultrasonic techniques. Ultrasonics 42, 1-9 (2004), 9-16
- [6] Davies, S.J., Edwards, C., Taylor, G.S., Palmer, S.B.: Laser-generated ultrasound: its properties, mechanisms and multifarious applications. J.Phys. D: Applied Physics 26(3) (1993), 329-348
- [7] Moreau, A., Lord, M.: High Frequency Laser-Ultrasonics. In: Green R.E. (eds) Nondestructive Characterization of Materials VIII, Springer, Boston, MA, 1998
- [8] Kundu, T.: Ultrasonic and Electromagnetic NDE for Structure and Material Characterization: Engineering and Biomedical Applications. CRC Press, London, 2016
- [9] Bass, H.E., Sutherland, L.C., Zuckerwar, A.J.: Atmospheric absorption of sound: Update. J. Acoust. Soc. Am. 88(4) (1990), 2019-2021
- [10] Fischer, B.: Development of an optical microphone without membrane. PhD thesis, Vienna University of Technology (2010)
- [11] Meschede, D.: Optics, Light and Lasers: The practical approach to modern aspects of photonics and laser physics. Wiley, 2007
- [12] Fischer, B., Rohringer, W., Panzer, N., Hecker, S.: Acoustic Process Control for Laser Material Processing. Laser Technik Journal 14(5) (2017), 21-25
- [13] Preisser, S., Rohringer, W., Liu, M., Kollmann, C., Zotter, S., Fischer, B., Drexler, W.: All-optical highly sensitive akinetic sensor for ultrasound detection and photoacoustic imaging. Biomedical Optics Express 7(10) (2016), 4171-4186
- [14] Lehmann, N., Jüttner, S.: Contribution to the qualification of air-coupled ultrasound as non-destructive, automated test method for spot welds in the car body shop. 15th APCNDT, Singapore (2017)
- [15] Clorennec, D., Prada, C., Royer, D.: Local and non-contact measurements of bulk acoustic wave velocities in thin isotropic plates and shells using zero group velocity Lamb modes. Journal of Applied Physics 101, 034908 (2007)